Computational Studies of Cu(II)/Met and Cu(I)/Met Binding Motifs Relevant for the Chemistry of Alzheimer's Disease

Rodolfo Gómez-Balderas, Duilio F. Raffa, Gail A. Rickard, Patrick Brunelle, and Arvi Rauk*

Department of Chemistry, University of Calgary, Calgary, Alberta T2N 1N4, Canada

Received: February 17, 2005; In Final Form: April 22, 2005

A systematic study of the binding motifs of Cu(II) and Cu(I) to a methionine model peptide, namely, *N*-formylmethioninamide **1**, has been carried out by quantum chemical computations. Geometries of the coordination modes obtained at the B3LYP/6-31G(d) level of theory are discussed in the context of copper coordination by the peptide backbone and the S atom of a methionine residue in peptides with special emphasis on Met35 of the amyloid-β peptide (Aβ) of Alzheimer's disease. The relative binding free energies in the gas phase, $\Delta G_{(g)}$, are calculated at the B3LYP/6-311+G(2df,2p)//B3LYP/6-31G(d) level of theory, and the solvation affects are included by means of the COSMO model to obtain the relative binding energies in solution, $\Delta G_{(aq)}$. A free energy of binding, $\Delta G_{(aq)} = -19.4$ kJ mol^{-1}, relative to aqueous Cu(II) and the free peptide is found for the most stable Cu(II)/Met complex, **12**. The most stable Cu(I)/Met complex, **23**, is bound by −15.6 kJ mol^{-1} relative to the separated species. The reduction potential relative to the standard hydrogen electrode is estimated to be $E°$(**12**/**23**) = 0.41 V. On the basis of these results, the participation of Met35 as a low affinity binding site of Cu(II) in Aβ, and its role in the redox chemistry underlying Alzheimer's disease is discussed.

Introduction

The pathogenesis of Alzheimer's disease (AD) is associated with the formation and subsequent deposition of amyloid-β peptide (Aβ), which is predominantly a 40−42 amino acid peptide. Although Aβ(1−42) is the primary component of brain amyloid deposits, both Aβ(1−40) and Aβ(1−42) can be found as soluble species in biological fluids. Much effort has been expended on identifying the pathways of Aβ metabolism because it could lead to alleviation routes of AD. Considerable evidence suggests that metals can interact directly with Aβ and may produce cerebral biometal dysregulation and oxidative stress[1,2] that are believed to be responsible for neuronal death.

Strong affinities have been found for Aβ with Cu(II), Zn(II), and to a lesser extent Fe(III).[3−5] In particular, for the complexation of Aβ(1−42) with Cu(II) at pH 7.4 in vitro, a high affinity site in the attomolar concentration range (log $K_{app} = 17.2$, $\Delta G_{(aq)} \approx -100$ kJ mol^{-1}) and a low affinity site in the nanomolar range (log $K_{app} = 8.3$, $\Delta G_{(aq)} \approx -47$ kJ mol^{-1}) have been identified.[6] The value of the affinity constant of Aβ(1−40) for Cu(II) is estimated to be in the picomolar range (log $K_{app} = 10.3$, $\Delta G_{(aq)} \approx -60$ kJ mol^{-1}).[6] Here, K_{app} is the pH-adjusted affinity constant. These values indicate that under biological conditions both Aβ(1−42) and Aβ(1−40) could complex Cu(II). However, lower affinities in the micromolar range, $\Delta G_{(aq)} \approx -35$ kJ mol^{-1}, but still sufficient to bind the metal, have also been reported for both Aβ(1−28)[7] and Aβ(1−40).[8] It has been suggested that discrepancies in the affinities reflect the existence of different binding modes.[7] Furthermore, there is evidence suggesting that Aβ(1−42) forms a dimer in Cu(II) solutions,[9] whereas the smaller Aβ(1−28) forms a one-to-one complex.[7] Thus, besides the different binding modes, peptide aggregation may contribute to the origin of discrepancies in the reported experimental values for the binding affinities.

Regarding the Cu(II)/Aβ coordination sphere in the high affinity site, the participation of His6, His13, and His14 present in the N-terminal (NT) of the peptide, and the N-terminus itself has been documented.[7] It is known that coordination of metals through His residues can result in conformational changes and aggregation of the peptide.[10] Participation of Tyr10 in the coordination sphere has been proposed,[11] but it is still controversial. For instance, although Tyr10 may be involved and play an active role in metal-catalyzed oxidation reactions, ^{1}H NMR studies in combination with CD spectra suggest that Tyr10 would not form part of the coordination sphere.[7] The participation of the backbone of the Aβ main chain in the Cu(II) coordination sphere is a contentious experimental issue. Features in the Raman spectrum of soluble Cu(II)/Aβ(1−42) have been associated with metal coordination of a deprotonated backbone amide nitrogen at neutral pH.[12] In contrast, Raman spectra of Aβ taken directly from senile plaque cores do not show this binding mode.[13] However, theoretical studies of Cu(II) binding to the His13/His14 Aβ region, actually show competitive binding between the nitrogen backbone and the carbonyl backbone.[14] Cu(II) ions are exchanged rapidly between peptides; consequently, it has not been possible to establish the coordination of Cu(II) for the low affinity sites.

The Aβ peptide contains a methionine (Met35) in the hydrophobic C-terminal (CT) domain. The complex between Cu(II) and Aβ has a relatively high reduction potential, $E° \approx 0.7$ V versus the standard hydrogen electrode.[15] It is thought that Met35 is key to the reduction of Cu(II) to Cu(I), with concurrent generation of elevated amounts of reactive oxygen species, H_2O_2 and OH$^\bullet$, which have been observed in cell culture and cell-free in vitro experiments.[15,16] Supporting the role of Met35, the Aβ(1−28) fragment, which lacks the methionine, failed to trigger redox activity to reduce Cu(II) despite the presence of the three His coordination sites in the peptide and the Tyr10 residue. Furthermore, when exogenous Met is added to Aβ(1−28), an enhancement of the Cu(II) reduction is

* To whom correspondence should be addressed. E-mail: rauk@ucalgary.ca.

10.1021/jp050843i CCC: $30.25
Published on Web 05/28/2005

observed.[17] However, the thermodynamics and mechanisms of the Cu(II)/Met binding and electron transfer are currently unclear. Recent results of Barnham et al.[18] suggest a second mode of neurotoxic activity of Aβ(1−42) independent of the Met residue, but leave the role of the Met unanswered when it is present.

Met35 can likely serve as an electron donor for the reduction of Cu(II) to yield Cu(I) and the radical cation $MetS^{\bullet+}$.[16,19] It has been shown that this radical cation can be stabilized by an amino[20,21] or phosphate group.[21−23] However, Met35 is rather distant from the His13/His14 high affinity binding site, and it may only reduce Cu(II) if the peptide is able to adopt a favorable conformation in which Met35 can reach the region where Cu(II) is found.

Given the importance of Cu(II)/Aβ interactions to the pathophysiology of amyloid deposition, it is desirable to study the copper binding affinities in specific regions of the peptide. The structural and energetic features of Cu(II)/Aβ complex formation can be investigated using suitable peptide models and quantum chemistry calculations. The results can provide relevant information about the relative stabilities of different binding motifs and affinities of specific regions of Aβ for Cu(II). The region around the Met35 site is an obvious region of interest because of the possibility of redox chemistry taking place.

In this work, the affinity of Cu(II) in aqueous solution for a small peptide region containing methionine has been investigated. The free energy in the gaseous phase and in aqueous solution of a number of Cu(II) and Cu(I) binding motifs with methionine have been calculated. The structural model for the peptide used in this investigation is *N*-formylmethioninamide **1** in the extended β-strand-like conformation. This simple model captures the methionine side chain and its closest protein-backbone surroundings and gives the possibility of studying copper coordination motifs that can involve backbone ligands as well as the sulfur. To study the Cu/Met binding motifs in aqueous solution, we explicitly included water molecules as part of the first coordination sphere of the copper. Finally, to discuss the role of the Met sulfur in the redox chemistry, we have also calculated the reduction potentials for the Cu(II)/Met complexes.

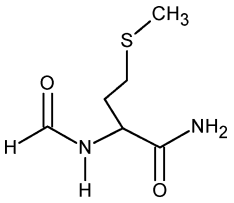

1

Computational Methods

Quantum chemistry calculations have been carried out using the Gaussian 98[24] and Gaussian 03[25] suites of programs. The Molden 4.0[26] and Molekel 4.0[27] visualization programs were employed extensively. Geometry optimizations were performed without geometry or symmetry constraints at the B3LYP/6-31G(d) level of theory. For each optimized structure, a frequency analysis at the same level of theory was used to verify that it corresponded to a stationary point on the potential energy surface. Frequencies scaled by 0.9806[28] were used to compute the zero-point vibrational energy; no scaling factor was used to calculate the thermal correction ($H_{298}° - H_0°$) or the vibrational entropies. Where necessary, the contributions of structural conformers to the gas-phase entropies have been taken into account, assuming that the gas is a mix of low lying conformers with the entropy of mixing approximated as $R\ln(n)$, where n is an estimate of the number of conformers.

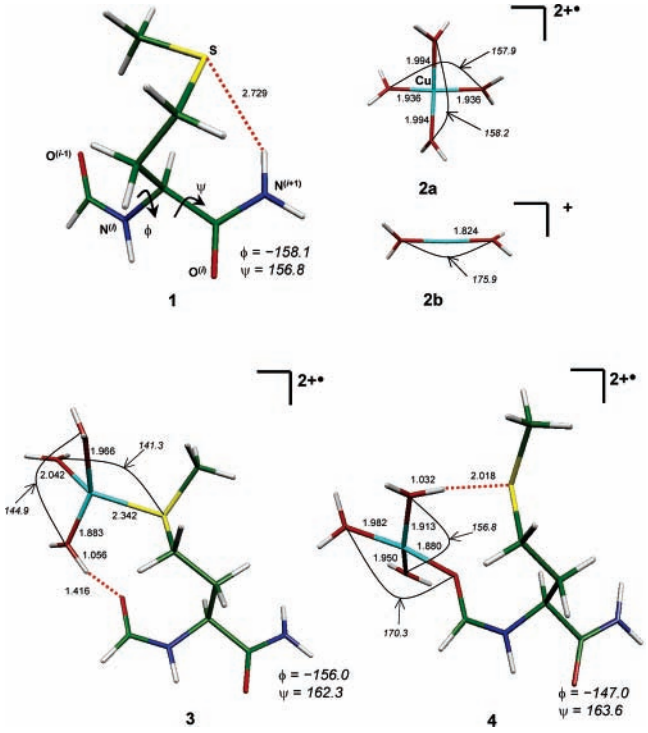

Figure 1. B3LYP/6-31G(d) optimized geometries of *N*-formylmethioninamide, **1**, $Cu(H_2O)_4^{2+}$, **2a**, $Cu(H_2O)_2^{+}$, **2b**, Cu(II) complexes of **1** with single coordination through the S atom, **3**, and through the amide carbonyl $O^{(i-1)}$, **4**. Distances in Å, bond angles and Ramachandran angles (ϕ and ψ) in degrees. Total charge and spin state are given.

More accurate ground-state energies were calculated at the B3LYP/6-311+G(2df,2p) level of theory to obtain reliable energy changes for the reaction pathways under study. Finally, the solvation energies (ΔG_{solv}), employed for the calculation of free energies of reaction in aqueous solution ($\Delta G_{(aq)}$), were obtained using the continuum COSMO[29] procedure as implemented in Gaussian 03 (SCRF = CPCM).[30,31] For the definition of the solvent cavity, the atomic radii were systematically adjusted to fit the molecular isodensity surface of 0.001 electrons $bohr^{-3}$.[32,33] To improve the computation of the thermodynamic parameters of our reactions, we have employed the experimental values of $\Delta G_{solv}(H_2O) = -26.4$ kJ mol^{-1} [34] and $\Delta G_{solv}(H^+) = -1107$ kJ mol^{-1} [35].

Results and Discussion

Free Peptide and Copper Aqueous Ions. The optimized structure of the most stable conformer of *N*-formylmethioninamide **1** is displayed in Figure 1. The oxygen atom of the formyl group, which would belong to the $i - 1$ residue, is labeled $O^{(i-1)}$, and the oxygen of the Met residue is labeled $O^{(i)}$. Likewise, the nitrogen from the Met residue is labeled $N^{(i)}$ and the nitrogen belonging to the $i + 1$ residue is labeled $N^{(i+1)}$. A number of different conformations (not shown) were tested in order to obtain the lowest energy geometry. Structure **1** is more stable by ca. 6 kJ mol^{-1} than the structure with the methionine side chain totally staggered and perpendicular to the backbone, possibly due to the intramolecular hydrogen bond between the amide N−H bond and the S atom. Ramachandran angles ϕ and ψ are shown in the Figures because they are used to discuss changes in the peptide backbone conformation that would favor copper chelation.

The Cu^{2+} ion is strongly solvated in aqueous solution and is often featured as the classic example of a transition metal with a 6-fold octahedral hydration shell. Because of its d^9 electronic configuration, a Jahn−Teller distortion[36] is generally assumed to axially elongate two bonds of the octahedral $Cu(H_2O)_6^{2+}$ complex, yielding a fast water exchange rate.[37] Ab initio molecular dynamics simulations on Cu(II) in water clusters indicate that because of the Jahn−Teller distortion, the Cu(II) ion loses one[38] or two[39] of the six water molecules from its octahedral coordination shell, producing either a loose trigonal bipyramidal or tetragonal pyramidal complex,[38] or a square planar one.[39] Ab initio computations, following the procedure described above, predict that $Cu(H_2O)_4^{2+}$ in a distorted square planar geometry is the most stable Cu(II)−aqua complex. Figure 1 presents the optimized structure, **2a**, for the $Cu(H_2O)_4^{2+}$ radical ion. Although complexes with five and six coordinated water molecules are stable in the gaseous phase, they are less stable than **2a** + H_2O/$2H_2O$ in the aqueous phase. As shown below, tetracoordinated Cu(II)/Met complexes are also more stable than higher-coordinated species where the additional coordination sites are filled by water.

At the present level of theory, the most stable Cu(I)−aqua complex is the bicoordinated species, **2b**, shown in Figure 1. It is essentially linear in structure, as is characteristic of many Cu(I) complexes.[40] A noticeable feature is the shorter Cu(I)−$O(H_2)$ bond distance, compared to Cu(II)−$O(H_2)$ in the more electrophilic, Cu(II)−aqua system. Unlike Cu(II)/Met complexes, which are most stable with the same number of coordinated ligands as the aqua complex, **2a**, some of the Cu(I)/Met complexes discussed below are more stable with higher coordination than complex **2b**.

Cu(II) Anchoring by the Peptide. Initial attachment of aqueous Cu(II) ion **2a** to the Met region of peptide **1** may occur by three different paths: (a) coordination through the sulfur atom; (b) coordination to the carbonyl oxygen atom ($O^{(i-1)}$), and (c) coordination to the carbonyl oxygen atom of the Met residue ($O^{(i)}$). In each case, the initial pentacoordinated Cu(II) structures were found to be less stable in water than the equivalent tetracoordinated species plus a solvated water molecule. Figure 1 displays the structures and relevant geometric parameters for coordination through the sulfur atom (complex **3**) and through the $O^{(i-1)}$ carbonyl (complex **4**). Efforts were made to anchor the copper involving only the $O^{(i)}$ carbonyl, but the optimization procedure converged to pentacoordinated complex **5** (Figure 2), where Cu(II) binds both carbonyl oxygen atoms. This structure will be discussed in the next section together with other 5-coordinate complexes. In both **3** and **4**, the copper coordination sphere takes a distorted square planar conformation, although attachment to $O^{(i-1)}$ gives a more planar metal center than attachment to sulfur. **3** and **4** are stabilized by a strong intramolecular hydrogen bond between a proton of one of the water molecules attached to the Cu(II), to $O^{(i-1)}$ in the case of **3**, and to sulfur in the case of **4**. The strength of these hydrogen bonds is evident from their rather short lengths, 1.42 Å in **3** and 2.02 Å in **4**, and from the elongated O−H bond in the water molecule involved. These values reflect the acidifying effect of Cu(II) on water. Clearly, binding motifs **3** and **4** retain the conformation of the original peptide backbone, that is, β strand: structure **3**, $\phi = -156.0°$, $\psi = 162.3°$; structure **4**, $\phi = -147.0°$, $\psi = 163.6°$.

Table 1 compiles gas-phase enthalpies, entropies (expressed as $-T\Delta S$), and Gibbs free energies for the Cu(II) reactions considered in this paper. The corresponding changes in the free energy for the solvation process as well as the final aqueous free energies are also included. These values can be derived from the data provided in Table S1 of the Supporting Information.

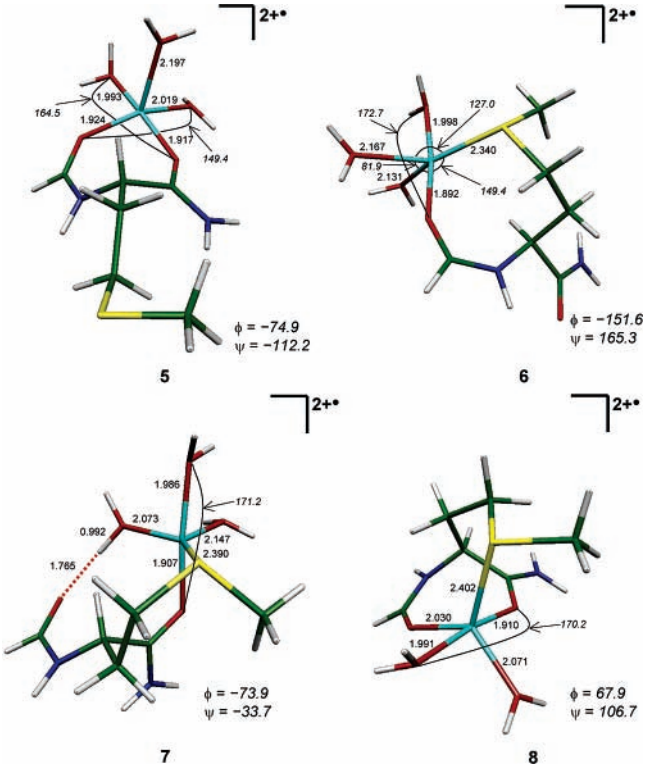

Figure 2. B3LYP/6-31G(d) optimized geometries of pentacoordinated Cu(II) complexes of **1** with more than one point of attachment. Distances in Å, bond angles and Ramachandran angles (ϕ and ψ) in degrees. Total charge and spin state are given.

TABLE 1: Thermodynamic Parameters (kJ mol^{-1}) for Complexation and Water Elimination of Cu(II)/Met in Gas Phase and Solution at $T = 298$ K

Cu(II) species	$\Delta H(g)^o$	$-T\Delta S(g)^a$	$\Delta G(g)^a$	$\Delta\Delta G_{solv}$	$\Delta G(aq)^a$
1 + **2a** → **3** + H_2O	−226.4	28.3	−198.1	205.5	7.4
1 + **2a** → **4** + H_2O	−229.0	23.1	−205.9	205.7	−0.2
4 → **5**	−16.0	−2.0	−18.0	49.2	31.2
4 → **6**	−22.8	7.1	−15.7	16.6	0.9
4 → **7**	−59.5	15.4	−44.1	40.0	−4.1
4 → **8** + H_2O	−18.0	−9.6	−27.7	20.3	−7.4
4 → **9** + H_2O	16.0	−18.0	−2.0	−8.1	−10.2
4 → **10** + H_2O	33.2	−16.7	16.5	−22.6	−6.1
4 → **11** + H_2O	10.4	−8.9	1.5	−12.3	−10.8
4 → **12** + $2H_2O$	53.7	−30.4	23.3	−42.5	−19.2
5 → **9** + H_2O	32	−16.0	16.0	−57.3	−41.4
6 → **10** + H_2O	56.0	−23.8	32.2	−39.2	−7.0
7 → **11** + H_2O	69.9	−24.3	45.6	−52.3	−6.7
8 → **12** + H_2O	71.8	−20.8	51.0	−62.8	−11.8
1 + **2a** → **12** + $3H_2O$	−175.3	7.3	−182.5	163.2	−19.4
1 + **2a** → **13** + H_2O + H^+	469.1	−11.2	457.9	−436.2	−18.3[b]
1 + **2a** → **14** + H_2O + H^+	488.4	−8.5	479.9	−383.5	56.4[b]

[a] The standard state is 1 M for all of the species, except H_2O, which is 55.6 M. [b] Values at pH = 7.

The formation of **3** and **4** corresponds to the displacement of water from the first coordination sphere of aqueous Cu(II) by a sulfide S atom and an oxygen atom of an amide, respectively. As seen in Table 1, the process is exergonic in the gaseous phase by ∼200 kJ mol^{-1}. However, this is entirely canceled by the loss of solvation of the small $Cu(H_2O)_4^{2+}$ complex, with the result that it is weakly endergonic in solution. The binding affinities for **3** and **4** differ by 7.6 and 7.8 kJ mol^{-1} in the gaseous phase and in solution, respectively.

The initial attachment of Cu(II) to the peptide is hindered in part by loss of freedom of the flexible Met side chain, for which 18 substantially populated conformers have been estimated.[21] In **3**, the side chain is restricted to $n = 2$ degrees of freedom. These originate from the attachment to one face or the other of the C−S−C plane (only one of these is shown in Figure 1). In **4** there is a H···S hydrogen bond in the gas phase that is not likely to be present when the species is in solution, leaving the Met side chain free to rotate. Therefore, $n = 9$ degrees of freedom (3×3 free rotations about the $^{\beta}$C−$^{\gamma}$C and $^{\gamma}$C−S 3-fold bonds) have been considered in the computation of the entropy for structure **4**, and for all those species where a H···S bond occurs in the optimized gas-phase structure. Subsequent additional points of attachment do not incur the entropic barrier. We examine some of these in the next section.

Geometries of the 5- and 4-Coordinated Cu(II) Complexes. Figure 2 depicts four different binding motifs for the secondary attachment of Cu(II) to the peptide, in which the Cu(II) ion is 5-coordinated: structure **5** (both carbonyl groups); structure **6** ($O^{(i-1)}$ and the sulfur atom); structure **7** ($O^{(i)}$ and the sulfur atom); and structure **8** (both carbonyl groups and the sulfur atom). The relevant geometric parameters for each species are also included in the Figure. In complex **5**, the copper center takes a square pyramidal geometry with the two carbonyls on the base and a loosely attached water molecule in the apical position ($r_{CuO} = 2.20$ Å). In **6**, **7**, and **8**, the metal center adopts a trigonal bipyramidal geometry with the sulfur atom in an equatorial position and oxygen atoms (from a carbonyl or a water molecule) in the axial positions (H_2O−Cu−O(=C) ≈ 170°). A strong preference of oxygen for axial positions in 6-coordinate cupric complexes has been reported for crystal structures[41] included in the Cambridge Structural Database. Attempts to optimize structures with the S atom in an axial position invariably resulted in its pseudorotation into an equatorial site.

Inspection of the bond distances for **6**, **7**, and **8** reveals that the equatorial ligands have longer distances than the ligands in axial positions. This suggests that the trigonal bipyramid geometry may be transformed readily into a square pyramidal complex by displacement of the axial and two of the equatorial ligands toward the same plane, whereas the remaining equatorial ligand ends up weakly bound, and prone to be eliminated, in the apical position (as in **5**).

Figure 3 shows the geometries for the tetracoordinated Cu(II) complexes, **9**−**12**. The Cu(II)−ligand bond distances and selected angles are displayed for each geometry. Resembling Cu(II) four-ligand cases **2a**, **3**, and **4**, discussed above, the metal center adopts a distorted square planar arrangement with planarity angles ranging from ∼136° to ∼160°. As expected, lower coordination produces shorter Cu(II)−ligand bond distances than those found in the pentacoordinated complexes. In particular, comparing **11** to **7**, as a consequence of the loss of coordination, the copper center exerts a stronger acidifying effect on the water molecules; thus, the hydrogen bond with the carbonyl is now slightly shorter. However, the average Cu−S bond distance in the 4-coordinated complexes, $r_{CuS} = 2.33$ Å, is slightly larger than the average value $r_{CuS} = 2.28$ Å of the tetracoordinate complexes reported[41] for crystal structures where the Cu−S bond occurs. In copper proteins, the active site generally holds two types of sulfur donors, a thiolate from a cysteine and a thioether group from an axial methionine[42] as well as nitrogen groups from histidines. Regarding the average copper−carbonyl oxygen distance, $r_{CuO} = 1.89$ Å, it is slightly shorter than the reported[41] average $r_{CuO} = 1.93$ Å occurring in crystal structures where Cu−O is present in the coordination sphere.

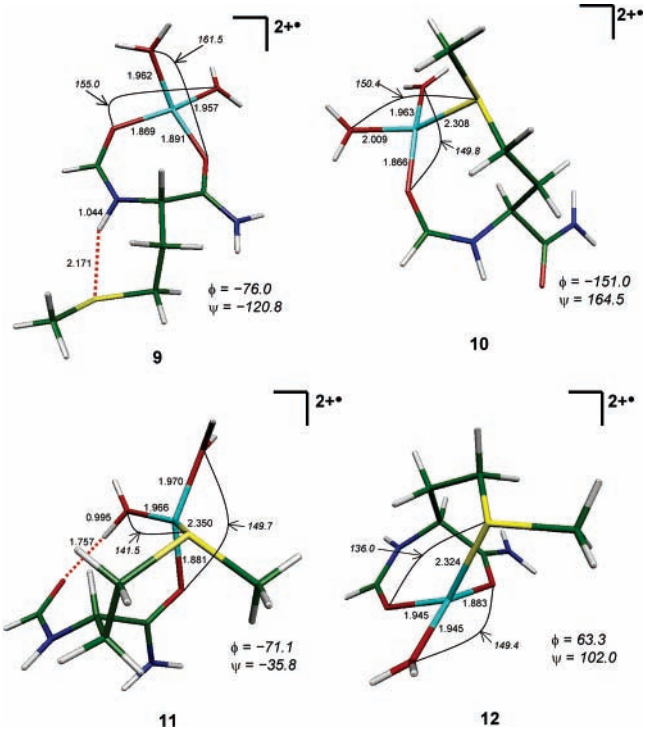

Figure 3. B3LYP/6-31G(d) optimized geometries of tetracoordinated Cu(II) complexes of **1** with more than one point of attachment.The most stable Cu(II) complex is **12**. Distances in Å, bond angles and Ramachandran angles (ϕ and ψ) in degrees. Total charge and spin state are given.

It is interesting to analyze the peptide ϕ and ψ Ramachandran angles (see Figures 2 and 3) because they indicate how the backbone conformation needs to be modified in order to bind Cu(II). To reach binding motif **5**, the peptide needs to adopt a coiled secondary structure with $\phi = -74.9°$ and $\psi = -112.2°$, significantly different from the β strand in **1.** In contrast, complex **6** accommodates its five ligands without considerable alteration of the Ramachandran angles, ending with $\phi = -151.6°$ and $\psi = 165.3°$. Thus, this binding motif may be reached easily if the peptide takes a β-sheet secondary structure. Regarding complex **7**, the peptide backbone angles are altered from the initial β strand in **1**, to $\phi = -73.9°$ and $\psi = -33.7°$, which correspond to an α helix. Finally, the Ramachandran angles of structure **8**, $\phi = 67.9°$ and $\psi = 106.7°$, indicate a second type of turn that can be taken by the polypeptide. Reduction of the coordination of **5**−**8**, by loss of water, to yield tetracoordinate complexes **9**−**12** (Figure 3) is not accompanied by significant alterations to the Ramachandran angles.

Relative Energies of the 5- and 4-Coordinated Cu(II) Complexes. All of the reported Cu(II)/Met energies hereafter are calculated with respect to complex number **4**, the most stable structure reached after single-point coordination of **1** to Cu(II). Use of structure **4** as a reference should lead to greater cancellation of residual errors in the calculated $\Delta\Delta G_{solv}$ values, and therefore yield more accurate relative free energies in solution.

Comparing the values of the free energies in the gaseous phase for the complexes in Figure 2, it is found that two or three chelating points give stabilization in all cases (see Table 1). Conversion of **4** to **7** has the greatest enthalpy and free energy changes, $\Delta H_{(g)}° = -59.5$ kJ mol^{-1}, $\Delta G_{(g)} = -44.1$ kJ mol^{-1},

indicating that **7** is the most stable pentacoordinated complex in the gas phase. The internal hydrogen bond between a Cu-bound water molecule and the $O^{(i-1)}$ contributes to this stabilization. In contrast, conversion of **4** with loss of water to form the triply chelated complex, **8**, is less favorable, $\Delta H_{(g)}^{\circ} = -18.0$ kJ mol^{-1}, although the gain in entropy adds to the free energy change in the gas phase, $\Delta G_{(g)} = -27.7$ kJ mol^{-1}. In all cases, conversion from **4** to produce **5**−**8** in aqueous solution is associated with a net loss in free energy of solvation, $\Delta\Delta G_{solv} \gg 17-49$ kJ mol^{-1}. This results in the binding energies of all pentacoordinated species being reduced when solvation effects are taken into account. The most exergonic process, formation of **8**, has $\Delta G_{(aq)} = -7.4$ kJ mol^{-1}.

Release of an equatorially (from the trigonal bipyramid) or apically (from the square pyramid) bound water molecule into solution to yield a distorted square planar complex (see Figure 3) is invariably an exergonic process. Loss of water from **5**, **6**, **7**, and **8**, yielding **9**, **10**, **11**, and **12**, gives $\Delta G_{(aq)} = -41.4$, -7.0, -6.7, and -11.8 kJ mol^{-1}, respectively (Table 1). These results indicate that the treatment of solvation effects associated with the fifth and sixth coordination sites of these Cu(II) complexes by means of the SCRF procedure is more accurate than the explicit treatment of adding water molecules to the first solvation shell. Similar effects are seen for the Cu(I) complexes discussed below, and are important in connection with the calculation of the Cu(II)/Met reduction potentials.

In contrast to conversion of **4** to produce **5**−**8**, gas-phase transformations of **4** to give the tetracoordinate complexes **9**−**12** (Figure 3) are now endothermic. In addition, the free energy change due to solvation becomes favorable. This negative $\Delta\Delta G_{solv}$ together with the entropy change results in values of $\Delta G_{(aq)}$ that favor the elimination of water in aqueous solution from **4** to yield structures **9**−**12**. The most exergonic process is that associated with forming **12** after removing two water molecules from **4**, with $\Delta G_{(aq)} = -19.2$ kJ mol^{-1}. Therefore, the calculated $\Delta G_{(aq)}$ relative to aqueous Cu(II) and the free peptide is -19.4 kJ mol^{-1}. The Ramachandran angles for **12** would indicate that this binding motif would be associated with a turn in the backbone of a polypeptide and may be hindered if other constraints impose β-strand or α-helix secondary structure. Structures **9**, **10**, and **11**, in which Ramachandran angles are compatible with such secondary structures, are just 9.0, 13.1, and 8.4 kJ mol^{-1}, respectively, less stable than **12**.

Aspects of Cu(II) Binding to the Nitrogens of the Backbone Amides. The ionization of backbone amide hydrogens normally occurs from pH 13 to 15 in peptides but is promoted in the presence of Cu(II) or Ni(II).[43] Hence, it is interesting to explore the binding of Cu(II) by the deprotonated nitrogens of model peptide **1**. Geometries and relative Gibbs free energies of tetracoordinated complexes, which include nitrogen from the backbone, were determined. Figure 4 displays binding motif **13**, where Cu(II) is chelated by sulfur and $N^{(i)}$, and **14**, where the Met sulfur and the $N^{(i+1)}$ nitrogen participate in the Cu(II) coordination sphere. Significant geometrical parameters are also given in the figure. The Cu−S bond distances $r_{CuS} \approx 2.36$ Å as well as Cu−O(H_2) distances are somewhat longer than those for species where the backbone oxygen is bound to copper instead of a deprotonated backbone nitrogen (see **10** and **11**).

Formation of **13** from the individual reactants is a highly endergonic process in the gas phase, with $\Delta G_{(g)} = 457.9$ kJ mol^{-1} (Table 1). However, the high cost in energy for deprotonation of $N^{(i)}$ is counterbalanced in solution by the significant free energy of solvation of the proton ($\Delta G_{solv} = -1107$ kJ mol^{-1}) [35] and the pH effect on the reaction (displacing the pH from 0 to 7 adds ~ -40.0 kJ mol^{-1}).[44] This results in an exergonic process with $\Delta G_{(aq)} = -18.3$ kJ mol^{-1}. As noted above, binding through $O^{(i-1)}$ to yield tetracoordinate complex **12** gives a $\Delta G_{(aq)}$ of -19.4 kJ mol^{-1}. Thus, **13** is predicted to have similar stability to **12** in solution at pH = 7.

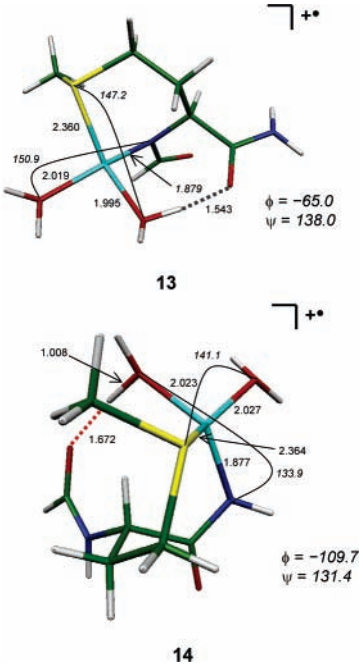

Figure 4. B3LYP/6-31G(d) optimized geometries of tetracoordinated Cu(II) complexes of **1** with deprotonated backbone nitrogen from the i (**13**) or the $i + 1$ (**14**) residue. Distances in Å, bond angles and Ramachandran angles (ϕ and ψ) in degrees. Total charges and spin state are given.

Similar to **13**, the calculated Gibbs free energy for conversion of the reactants to produce **14** in the gas phase is highly endergonic, $\Delta G_{(g)} = 479.9$ kJ mol^{-1}. However, unlike **13**, the free energy change in solution is now endergonic, $\Delta G_{(aq)} = 56.4$ kJ mol^{-1}. This is due to a higher gas-phase enthalpy and less solvation stabilization for **14** compared to **13** (Table S1).

Cu(II) Binding Affinities, Implications for Aβ. As discussed above, a low affinity site for the binding of Cu(II) to Aβ in the order of micromolar concentrations, that is, $\Delta G_{(aq)} \approx -35$ kJ mol^{-1}, has been discovered.[7] We consider here whether the Met35 region of Aβ may serve as that site. The most stable complexes between **1** and aqueous Cu(II) are **12** and **13**, for which $\Delta G_{(aq)} \approx -19$ kJ mol^{-1}. Previous work carried out in this group has indicated that an amino group will displace water from the coordination sphere of Cu(II) in an exergonic process.[45] Thus, involvement of the N-terminus or the side chains of Lys28 or Lys16 in place of the single coordinating water of **12** or by displacing a water molecule from **13** may well raise the binding affinity into the observed range. Indeed, the same is true in the case of **10** and **11**, both of which involve Cu(II) coordination to the sulfur of Met35. It is also true of structure **9**, which does not have the S atom in the coordination sphere, and therefore may represent binding to any residue of Aβ, or indeed of any protein. However, structures **10**−**13** have special significance because they provide the opportunity of a direct role for the Met residue in the reduction of the Cu(II). Structure **10**, although having the smallest binding affinity of the tetracoordinate structures in Figure 3 with $\Delta G_{(aq)} \approx -6$ kJ mol^{-1}, is unique in that the backbone of the peptide retains the geometry required of a β strand and may be part of a β sheet. The reduction chemistry of Cu(II)/Met will be explored after consideration of the structure and stability of Cu(I) complexes with **1**.

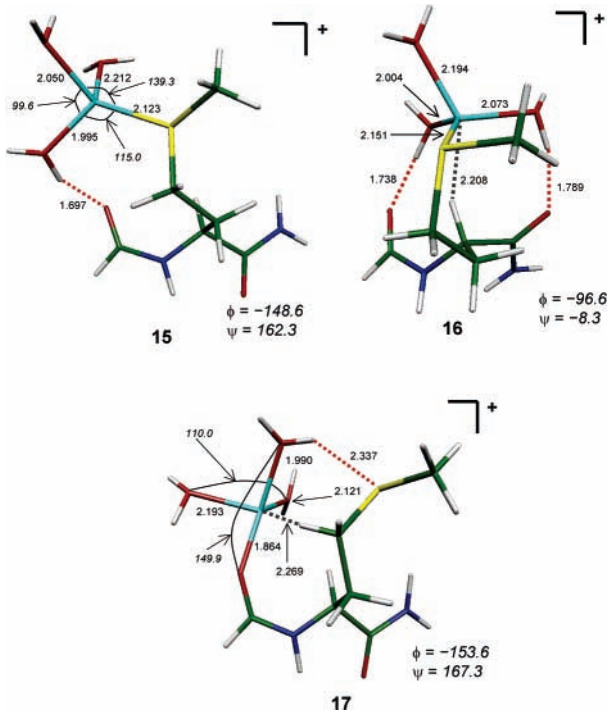

Figure 5. B3LYP/6-31G(d) optimized geometries of tetracoordinated Cu(I) complexes of **1** with more than one point of attachment. Distances in Å, bond angles and Ramachandran angles (ϕ and ψ) in degrees. Total charges are given.

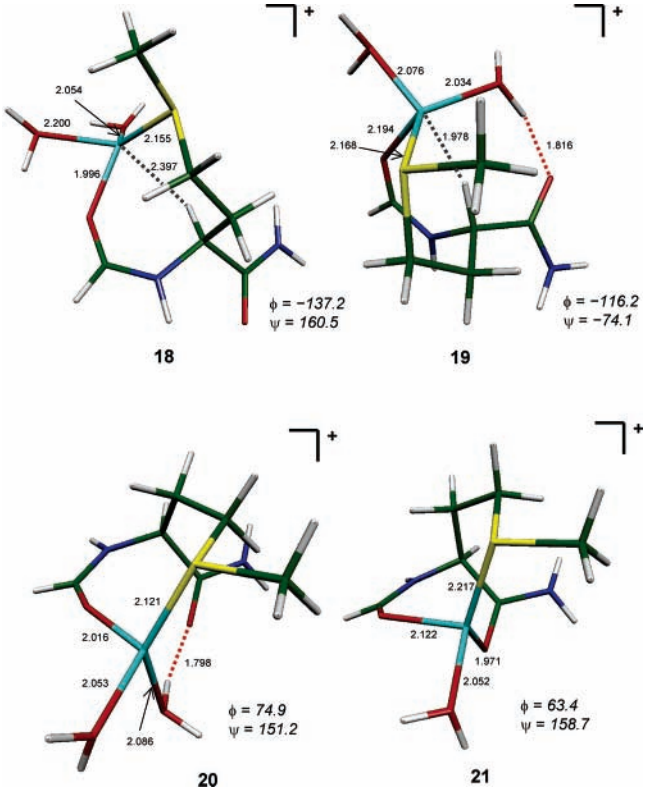

Figure 6. B3LYP/6-31G(d) optimized geometries of tetracoordinated Cu(I) complexes of **1** with more than one point of attachment. Distances in Å, and Ramachandran angles (ϕ and ψ) in degrees. Total charges are given.

Cu(I) Anchoring by the Peptide. Tetracoordinated Cu(I)/Met structures were obtained by the addition of an electron to the Cu(II) structures discussed above, as well as from several other starting points. All are local mimima in the gaseous phase. Figure 5 shows the tetracoordinated Cu(I)/Met complexes with $Cu(H_2O)_3^+$ anchored at one point of peptide **1** by the sulfur atom in **15** and **16** and by $O^{(i-1)}$ in **17**. Selected geometrical parameters are included for each species. In S-coordinated structure **15**, the ligands of Cu(I) are arranged approximately tetrahedrally, and there is a short intramolecular hydrogen bond (1.70 Å). Cu(I) is a d^{10} metal, and the acidifying effect on the bound water molecules is less than that of Cu(II). For instance, structure **3** (Figure 1) has a markedly shorter intramolecular hydrogen bond, H···O is 1.40 Å. Moreover, in **15**, the Cu−S distance is shortened from 2.34 (in **3**) to 2.12 Å, whereas all three Cu−O distances are longer than those in the oxidized form. Remarkably, in structures **16** and **17**, the ligands are arranged in a trigonal bipyramidal manner, the fifth coordination site being occupied by the H atom of the $^{\alpha}$C and $^{\gamma}$C atoms, respectively. Such possible agostic interactions, previously reported for Cu(I) complexes,[46,47] have been investigated in this work for structure **19** (vide infra), which shows the shortest Cu···H bond distance.

Multiple Attachment of Cu(I) to 1. Tetracoordinated structures **18**−**21** in which the Cu(I) is bound to more than one atom of **1** are presented in Figure 6. Significant bond distances are also given. In these motifs, the metal center adopts a distorted tetrahedral geometry. As in the case of **16** and **17**, structure **19** has a remarkably short distance between the hydrogen of a C−H bond and the metal center, Cu···H = 1.98 Å. Such an agostic Cu···H($^{\alpha}$C) interaction is expected to red-shift the stretching frequency of the affected H−C bond.[48] For instance, the agostic interactions between Cu(I) and methyl-group hydrogens, in Cu(I)/propane complexes, shift the methyl H−C harmonic frequency by 470 cm^{-1}.[46] This is not the case in the present systems. The H−$^{\alpha}$C bond stretching frequency in free peptide **1** is calculated to be 3094 cm^{-1}, whereas the corresponding value in **19** is 3092 cm^{-1}. Likewise, natural bond orbital (NBO)[49] population analysis shows negligible charge transfer from the hydrogen to the metal, specifically q(Cu) = 0.81 and q(H($^{\alpha}$C)) = 0.20 in **19** are comparable with q(Cu) = 0.82 and q(H($^{\alpha}$C)) = 0.22 in **20** where, because of the conformation, the Cu···H interaction is absent.

Relative Energies of 4-Coordinate Cu(I) Complexes. Table 2 contains the relative thermodynamic parameters for complexation of Cu(I) to **1**. All of the primary data are included in Table S1 of the Supporting Information. In aqueous solution, structure **15** is more stable than **16** by 11.2 kJ mol^{-1}, and more stable than **17** by 52.0 kJ mol^{-1}. Thus, the two structures in which Cu(I) is directly coordinated to S are significantly more stable than **17** in which coordination is solely to an amide oxygen atom. This is in contrast to **3** (Cu(II)−S coordination) and **4** (Cu(II)−$O^{(i-1)}$ coordination) that differ in free energy by less than 8 kJ mol^{-1} (Table 1). These results support a preference for Cu(I) binding sulfur instead of an amide carbonyl oxygen.

Structures **18**−**20** (Figure 6) differ from **15** (Figure 5) by replacement of a water molecule by the $O^{(i-1)}$ atom. Structure **21** represents displacement of two molecules of water and the coordination of both amide oxygen atoms. Although all are local minima, none of these structures are more stable in the gaseous phase than **15**. The enthalpy changes for the substitution reactions (see Table 2) reflect the energy cost of removing water molecules from **15**, $\Delta H_{(g)}^{\circ}$ are positive by ∼25 to ∼115 kJ mol^{-1}. Even after adding the positive changes in entropy, the free energy changes are still positive; $\Delta G_{(g)}$ varies from ∼7 to ∼80 kJ mol^{-1}. However, the free energy changes due to solvation are negative by approximately the amount gained by the solvation of each released water molecule ($\Delta G_{solv}(H_2O)$ = −26.4 kJ mol^{-1}). In aqueous solution, the most stable tetra-

TABLE 2: Thermodynamic Parameters (kJ mol^{-1}) for Complexation and Water Elimination of Cu(I)/Met in Gas Phase and Solution at $T = 298$ K

Cu(I) species	$\Delta H_{(g)}{}^{o}$	$-T\Delta S_{(g)}{}^{a}$	$\Delta G_{(g)}{}^{a}$	$\Delta\Delta G_{solv}$	$\Delta G_{(aq)}{}^{a}$
1 + **2b** → **15**	−173.0	−65.7	−107.3	128.6	21.3
15 → **16**	−11.0	10.6	−0.4	11.7	11.2
15 → **17**	46.6	−5.1	41.6	10.5	52.0
15 → **18** + H_2O	25.2	−18.1	7.1	−20.9	−13.8
15 → **19** + H_2O	29.4	−12.9	16.5	−21.5	−5.0
15 → **20** + H_2O	53.5	−22.3	31.2	−14.5	16.7
15 → **21** + $2H_2O$	114.6	−34.3	80.3	−47.3	33.0
15 → **22** + H_2O	24.0	−21.5	2.5	−21.1	−18.6
15 → **23** + $2H_2O$	54.9	−38.5	16.4	−53.4	−37.0
15 → **24** + H_2O	52.6	−26.1	26.5	−18.7	7.8
15 → **25** + $3H_2O$	133.9	−57.1	76.8	−84.2	−7.4
17 → **24** + H_2O	6.0	−21.0	−15.1	−29.2	−44.2
18 → **23** + H_2O	29.7	−20.4	9.3	−32.5	−23.2
21 → **25** + H_2O	19.3	−22.8	−3.5	−36.9	−40.4
23 → **26** + H_2O	99.9	−20.5	79.4	25.9	105.2
23 → **27**	94.2	−6.6	87.6	−37.4	50.2
1 + **2b** → **23** + H_2O	−118.0	−27.2	−90.8	75.2	−15.6
1 + **2b** → **28** + H_2O + H+	961.4	2.9	964.3	−867.9	56.5[b]
1 + **2b** → **29** + H_2O + H+	938.4	4.8	943.1	−856.7	46.4[b]

[a] The standard state is 1 M for all of the species, except H_2O, which is 55.6 M. [b] Values at pH = 7.

coordinated structure is **18**. Release of water from **15** to yield **18** is predicted to be exergonic, by 13.8 kJ mol^{-1}.

The only species in which the backbone remains in the extended (β-strand) conformation, as in **1** and **15**, is the most stable tetracoordinated structure, **18**. It is possible to attribute part of the relative instability, of say **19**, to the strain energy required to change the amino acid backbone angles from those of the stable extended conformation in **18** ($\phi = -137.2°$, $\psi = 160.5°$) to the Ramachandran angles of **19** ($\phi = -116.2°$, $\psi = -74.1°$). The difference in the energy of **18** and **19**, with the $Cu(H_2O)_2{}^{+}$ moiety removed is 27.9 kJ mol^{-1} in the gas phase, favoring **18**. These results indicate that a β-sheet-like conformation in the methionine region would retain Cu(I) more easily than the coiled structures.

Tricoordinate Cu(I)/Met Structures. For small Cu(I) complexes at the same level of theory employed here, aqueous Cu(I) is most stable when coordinated to two ligands, for example, structure **2b** (Figure 1)[45] rather than to three or four ligands. Consequently, it was anticipated that the aqueous Cu(I)/Met complexes would have lower coordination at copper than Cu(II)/Met complexes and that the Cu(I) complexes discussed above would prefer to release one or more waters. Structures with lower coordination were located by systematically removing water molecules from the gaseous-phase Cu(I) species, **15**−**21**, and allowing one, two, or three coordination points in the peptide.

Figure 7 shows 3-coordinated optimized Cu(I)/Met structures **22**−**25**, with selected bond distances as well as bond angles given. From the sum of the angles at Cu(I), that is, close to 360°, one can see that these complexes adopt a nearly planar geometry at the metal. Bond distances are shortened after removing one ligand, as can be seen from comparison with the corresponding tetracoordinated complexes. The average Cu−S bond distance $r_{CuS} = 2.12$ Å, is slightly shorter than the average value, $r_{CuS} = 2.26$ Å of 3-coordinated Cu(I) crystal structures.[41] Complex **24** exhibits a T-shape coordination, which has also been found in previous theoretical studies for the $Cu(H_2O)_3{}^{+}$ ion.[50]

Structures **22**−**25** may be derived directly from **15**, **17**, **18**, and **21**, respectively, by the removal of a water molecule. As expected, each of these processes is exergonic in aqueous solution, by ∼19 to ∼44 kJ mol^{-1} (Table 2). From the relative

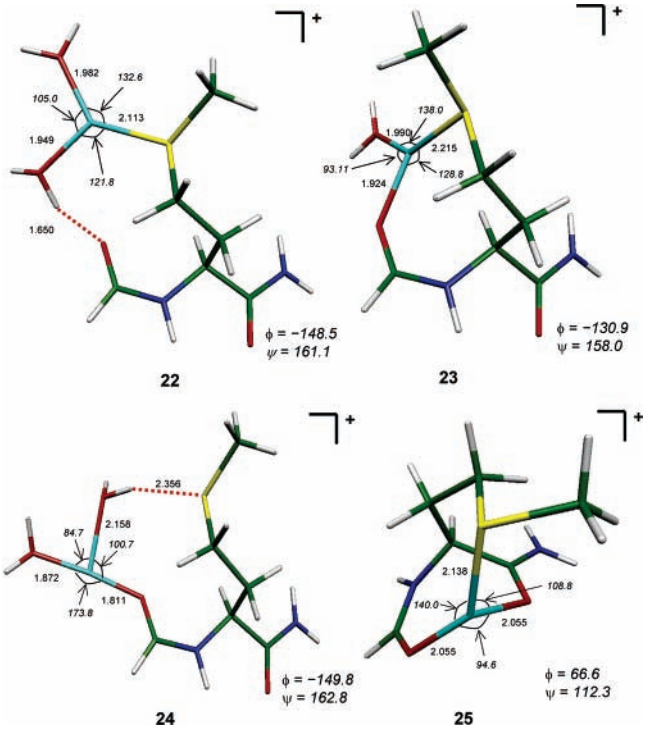

Figure 7. B3LYP/6-31G(d) optimized geometries of tricoordinated Cu(I) complexes of **1** with more than one point of attachment. The most stable Cu(I) complex is **23**. Distances in Å, bond angles and Ramachandran angles (ϕ and ψ) in degrees.

stabilities given in Table 2 with respect to **15**, it can be seen that the most stable Cu(I)/Met structure in solution is **23**. The stability of **23** with respect to the Cu(I) aqueous ion, **2b**, and the free peptide, **1**, is computed to be −15.6 kJ mol^{-1}.

Dicoordinated Cu(I) Structures. As has been discussed above, at the present level of theory and treatment of solvation, small Cu(I) complexes prefer a linear geometry with two ligands, similar to **2b** (Figure 1).[45] However, this is not the case for the complexes with methionine. When the water molecule is removed from tricoordinated **23**, product **26** (Figure 8) is 105.2 kJ mol^{-1} less stable in solution. Similarly, with the release of the weakly bound water molecule from **24**, the optimization procedure converges either to the most stable structure, **23**, or to complex **27** (Figure 8) with two hydrogens from the methionine side chain forming part of the copper coordination sphere. In aqueous solution, **27** is less stable than **23** by 50.2 kJ mol^{-1}.

Aspects of the Cu(I) Binding Process to the Nitrogens of the Backbone Amides. As in the case of Cu(II), the participation of the $N^{(i)}$ or $N^{(i+1)}$ deprotonated nitrogens in the coordination sphere of Cu(I) has been studied. Tricoordinated structures were used as starting points for the optimization process. Structure **28**, in which coordination is to $N^{(i)}$, shows a long Cu(I)−S bond length, $r_{CuS} = 2.88$ Å with S in an axial position of the T-shaped complex (Figure 8). It is worth noting that a long axial Cu(I)−S(Met) bond length of ∼2.9 Å is a common feature in blue copper proteins.[42] Structure **29** corresponds to a Cu(I) center with only two ligands, $N^{(i+1)}$ and a water molecule. In this case, the Met sulfur is released from the metal coordination sphere. Efforts to locate a minimum energy tricoordinated structure with deprotonated nitrogen and Met sulfur ligands consistently resulted in sulfur being liberated.

Gibbs free energies for **28** and **29** relative to the free reactants are given in Table 2. In both cases, the complexation process is highly endergonic in aqueous solution at pH = 7, with $\Delta G_{(aq)}$

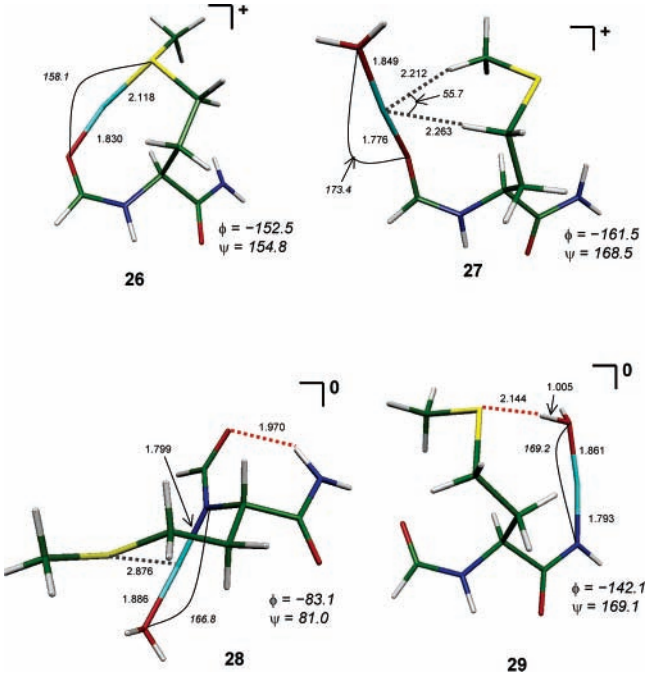

Figure 8. B3LYP/6-31G(d) optimized geometries of dicoordinated Cu(I) complexes of **1**. Distances in Å, bond angles and Ramachandran angles (ϕ and ψ) in degrees. Total charges are given.

$= 56.5$ kJ mol^{-1} for **28** and $\Delta G_{(aq)} = 46.4$ kJ mol^{-1} for **29**. Thus, complexes with coordination of Cu(I) to the backbone nitrogen amide are unlikely to be formed in solution.

Reduction Potentials. *Considerations in the Calculation of Reduction Potentials, E°.* The calculation of reduction potentials, *E*, relative to the standard hydrogen electrode, for the Cu(II)-containing species is accomplished via eq 1

$$E^\circ(\text{“Cu(II)”}/\text{“Cu(I)”}) = -\frac{\Delta G_{(aq)}}{F} \qquad (1)$$

where “Cu(II)” and “Cu(I)” represent specific species containing oxidized and reduced copper, respectively, *F* is the Faraday constant ($F = 96.485$ kJ mol^{-1} V^{-1}), and $\Delta G_{(aq)}$ is the aqueous free energy for reaction 2

$$\text{“Cu(II)”} + {}^1/_2H_{2(g)} \rightarrow \text{“Cu(I)”} + H^+_{(aq)} \qquad (2)$$

For most of the energy differences calculated in the previous sections, errors inherent in the calculation of the absolute values could be expected to cancel, yielding reliable relative energies. This is not the case for the calculation of aqueous free energy changes for reactions like eq 2. Because a transition element is involved and the number of electrons changes, the enthalpy change will be less accurately described at this theoretical level than expected for lighter elements. For instance, the calculated ionization potential of Cu^+ (i.e., the second ionization potential of atomic copper) is $IE_2^{calcd} = 2008$ kJ mol^{-1}, whereas experiment gives $IE_2^{exptl} = 20.29$ V (1958 kJ mol^{-1}).[51] The discrepancy, 50 kJ mol^{-1}, is probably due to the unequal treatment of electron correlation (an enthalpic term). We assume that the error in the ionization potential of Cu^+ will be present in the reduction potentials, E°(“Cu(II)”/“Cu(I)”), irrespective of the metal environment because they will all involve the change in copper oxidation state from +2 to +1. Consequently, 50 kJ mol^{-1} has been added to the gaseous phase, $\Delta H_{(g)}$ (Table 3), and appears in the free energies for computing the reduction potentials.

The problem is compounded by the change in charge in eq 2, which aggravates errors inherent in the calculation of $\Delta\Delta G_{solv}$ values due to deficiencies in the solvation model. In partial compensation, we use the experimental value for the free energy of solvation of the water, $\Delta G_{solv}(H_2O) = -26.4$ kJ mol^{-1},[34] and proton, $\Delta G_{solv}(H^+) = -1107$ kJ mol^{-1}.[35] We also adopt the experimental value for the “hydrogen” half reaction, ${}^1/_2H_2 \rightarrow H^+ + e^-$, $\Delta G_{(g)} = 418$ kJ mol^{-1}.[52] Thus, the calculation of E° for the aqueous cupric ion, namely, reaction 3

$$Cu(H_2O)_4^{2+} + {}^1/_2H_{2(g)} \rightarrow Cu(H_2O)_2^{+} + H^+_{(aq)} + 2H_2O \qquad (3)$$

yields $E^\circ(Cu(H_2O)_4^{2+}/Cu(H_2O)_2^{+}) = 0.44$ V (Table 3), which has to be compared to the experimental value of 0.17 V.[51] The remaining difference, 0.27 V (26 kJ mol^{-1}), arises primarily from the calculation of the free energy of solvation for both the Cu^{2+} and Cu^+ ions. It will probably be less in the case of the Cu/Met complexes because the Cu ions are more shielded from the continuum model by ligands other than water, and the values of ΔG_{solv} are much smaller in absolute magnitude than for **2a** and **2b** (see Table S1). In summary, in the calculation of Cu(II)/Met reduction potentials reported in Table 3 and discussed below, we have applied the correction arising from the ionization energy of the copper. We have *not* applied a correction due to the solvation of the aqueous copper complexes but take note of the fact that the calculated values will be overestimated by some amount less than 0.27 V.

Cu(II)/Met Reduction Potentials. The metal-catalyzed one-electron oxidation of methionine to yield the methionine sulfide radical cation $MetS^{\bullet+}$ [16,19] is believed to play an important role in the oxidation of Aβ during the pathogenesis of Alzheimer's disease.[22,53] However, the relevant thermodynamics and the mechanism of the process are still unknown. In this section, some reduction potentials for selected Cu(II)/Met complexes have been computed. The results are discussed in terms of the stabilizing/destabilizing contribution of the solvent, backbone carbonyl and Met sulfur ligands, and the consequences of secondary structure imposed by the polypeptide chain.

The reduction potential for some relevant combinations of “Cu(II)”/“Cu(I)” pairs are reported in Table 3. In particular, for the most stable Cu(II) species, **12**, producing the most stable Cu(I) species, **23**, the calculated value is E°(**12**/**23**) = 0.41 V. This number is similar to the value of 0.44 V calculated for the aqueous Cu^{2+} ion. Bearing in mind that the latter is an overestimate and the former is likely to be also, we conclude that E°(**12**/**23**) is not distinguishable from the reduction potential of an aqueous Cu^{2+} ion. In fact, desolvation effects, that is, reduction in the number of water molecules around the metal center, of protein copper sites have been held to be responsible for raising the reduction potential compared to that of the aqueous Cu^{2+}/Cu^+ pair. This is mainly due to a net stabilization of the less charged Cu(I) oxidation state.[54,55] A tentative conclusion is that the process associated with the high measured reduction potential of Cu(II)/Aβ = 0.7 V[15] is not that modeled by **12** → **23**.

Effect of Available Ligands on *E*°. Several other values of reduction potentials are listed in Table 3. The effect of Cu(II) binding only to S may be gauged from the reduction potential of structure **3** (Figure 1), E°(**3**/**22** + H_2O) = 0.49 V. This value is somewhat higher than that for the reduction of **12** or aqueous Cu^{2+} **2a** and indicates that the S atom of the Met is a better ligand for Cu^+ than it is for Cu^{2+}. In a similar vein, structure **4** (Figure 1) models the case where the Cu^{2+} is bound only to the carbonyl of an amide group. Its reduction, yielding **24** (Figure 7), has E°(**4**/**24** + H_2O) = 0.14 V. This is substantially

TABLE 3: Thermodynamic Data (kJ mol^{-1}) and Reduction Potentials (V) for "Cu(II)"/"Cu(I)" Pairs in Solution at T = 298 K

reduction process	$\Delta H(g)^o$	$-T\Delta S_{(g)}$ [a]	$\Delta G(g)$ [a]	$\Delta\Delta G_{solv}$	$\Delta G_{(aq)}$ [a]	E^o [b]
2a → **2b** + 2H_2O	511.8	−48.5	463.3	−498.1	−42.8	0.44[c]
3 → **22** + H_2O	589.2	−32.6	556.6	−596.1	−47.5	0.49
3 → **23** + 2H_2O	620.1	49.6	570.5	−628.5	−65.9	0.68
4 → **23** + 2H_2O	622.7	44.4	578.3	−628.7	−58.3	0.60
10 → **23** + H_2O	589.5	−27.7	561.9	−606.2	−52.3	0.54
12 → **23**	569.0	−14.0	555.0	−586.3	−39.3	0.41
13 + H^+ → **23** + H_2O	−75.3	29.8	−45.5	13.1	−40.4	0.83 (0.42)[d]
4 → **24** + H_2O	620.4	−32.0	588.4	−594.0	−13.6	0.14
9 → **25** + 2H_2O	685.8	45.0	640.7	−651.4	−18.7	0.19
12 → **25** + H_2O	548.0	−32.6	615.3	−617.1	−9.8	0.10
13 → **28** + H_2O	1004.1	34.4	969.7	−929.9	31.7	−0.33
14 → **29** + H_2O	961.8	35.2	926.5	−971.5	−52.9	0.55

[a] The standard state of all species corresponds to 1 M, except for H_2O, which is 55.6 M and $[H^+] = 10^{-7}$ M. [b] Values with respect to the standard hydrogen electrode. [c] The experimental value for the Cu^{2+}/Cu^+ pair is 0.17 V. See the discussion about the corrections in the text. [d] $E^{o'}$ value in parentheses, $E^{o'} = E^o - 0.41$ V at pH = 7 because amide p$K_a \gg 7$.

lower than that of **2a** and indicates that the carbonyl oxygen atom is not as good a ligand for Cu^+ as it is for Cu^{2+}. In structure **9**, the Cu^{2+} is coordinated to two carbonyl groups but not to the S atom. Reduction of **9** does not yield a comparable Cu^+ structure. During the course of the optimization of the reduced complex, the S atom becomes coordinated to the Cu^+, yielding structure, **25**, after loss of water, $E°$(**9**/**25** + H_2O) = 0.19 V. In structure **12**, the Cu(II) is coordinated to both carbonyls and the S. The coordination pattern is the same as that of the reduced compound, **25**, $E°$(**12**/**25** + H_2O) = 0.10 V. In summary, coordination of Cu(II) to two carbonyls rather than water is associated with lower reduction potentials than for free cupric ions.

Effect of Secondary Structure on $E°$. Structures **9** or **12** are compatible with Cu(II) binding to a turn region of the polypeptide (ϕ, ψ angles in Figure 3). If the peptide is constrained by secondary structure to be in a β strand (e.g., structure **1**, Figure 1) or β sheet, the Cu(II) coordination may be modeled by structures **3**, in which the Cu(II) is coordinated only to the S atom, **4**, in which coordination is only to a carbonyl, and **10**, in which the Cu(II) is chelated by both the S atom and the $O^{(i-1)}$ carbonyl. Structure **10** is less stable than the most stable Cu(II) structure, **12**, by about 13 kJ mol^{-1}. Reduction of **10** yields, directly, the most stable Cu(I) complex, **23**, after loss of water. The reduction potential for this process is $E°$(**10**/**23** + H_2O) = 0.54 V. Structure **23** may also be the product of reduction of **3** and **4**, which are higher in energy than **10** by 13.7 and 6.1 kJ mol^{-1}, respectively. The corresponding reduction potentials are, $E°$(**3**/**23** + H_2O) = 0.68 V and $E°$(**4**/**23** + H_2O) = 0.60 V. The higher $E°$ values reflect the less than ideal coordination configurations of Cu(II) relative to Cu(I).

Effect of Backbone Nitrogen Coordination on $E°$. Finally, we examine the reduction of the two structures, **13** and **14** (Figure 4), in which the Cu(II) is coordinated to a deprotonated backbone amide N atom. As discussed above, structure **13** is predicted to coexist with the most stable Cu(II) structure, **12**, at pH = 7. Reduction of **13** while retaining coordination to the deprotonated amide, $N^{(i)}$, yields structure **28** (Figure 8) in which the S atom also has a weak interaction with the nominally dicoordinated Cu(I). For this process, $E°$(**13**/**28** + H_2O) = −0.33 V. The low value reflects the instability of the deprotonated Cu(I) complex, **28**, which is predicted to be unstable toward dissociation and reprotonation by 56.5 kJ mol^{-1} (Table 2). For the case where **13** is reduced yielding the most stable Cu(I) structure, **23**, in which the amide backbone is reprotonated, $E°'$(**13** + H^+/**23** + H_2O) = 0.42 V (pH = 7).

Structure **14** involves Cu(II) coordination to the deprotonated nitrogen of the formally $i + 1$ residue, forming a 7-membered ring. The reduction potential of **14** yielding the equivalent Cu(I) complex, **29**, in which the S is no longer coordinated, has $E°$(**14**/**29** + H_2O) = 0.55 V. Structure **14** is only of academic interest because it is predicted to be unstable relative to **1** + **2b** by 56 kJ mol^{-1}. It is included here only for completeness.

Conclusions

In this paper, several binding motifs for Cu(II) and Cu(I) with *N*-formylmethioninamide **1**, a model for a methionine residue in a peptide, have been presented. Tetracoordinate Cu(II)/Met complexes are more stable than those with higher coordination numbers at the B3LYP/6-311+G(2df,2p)//B3LYP/6-31G(d) + CPCM level of theory. Binding motifs **12** and **13** are found to be stable by ca. 19 kJ mol^{-1} in aqueous solution. This implies that Cu(II) chelation through the carbonyl groups and sulfur atom in **12** is competitive with $N^{(i)}$-ionized α-amino group **13** at pH 7. Complex **10**, which is ∼13 kJ mol^{-1} less stable, has Cu(II) bound to the peptide in a β-strand-like conformation. For Cu(I)/Met, the tricoordinate complexes are more stable than the tetracoordinate or bicoordinate species. The most stable Cu(I)/Met species, **23**, has a computed affinity of ca. −16 kJ mol^{-1}. Unlike Cu(II)/Met, Cu(I)/Met complexes in which the metal is coordinated to a deprotonated backbone amide N atom are not likely to be formed in solution.

The reduction potentials of a number of complexes between Cu(II) and **1** were calculated with two objectives in mind. First, the effects of different combinations of S, O, and N ligands on the reduction potential were examined to see whether they would raise or lower the reduction potential relative to that of aqueous Cu^{2+}, for which $E°(Cu^{2+}/Cu^+)$ = 0.17 V versus the standard hydrogen electrode.[51] It was found that coordination only by S (and water) led to a slight raising of $E°$ (by ∼0.1 V), whereas coordination by one or two amide carbonyl O atoms led to a lowering of $E°$ (by 0.2 V − 0.3 V). Coordination of both the Cu^{2+} and Cu^+ by the deprotonated amide N atom resulted in negative values of $E°$ (a lowering of ∼0.5 V). Second, because some of the complexes could serve as models for the binding of Cu(II) in the Met35 region of Aβ, comparison of the calculated reduction potentials with the experimental value for Cu(II)/Aβ, 0.7 V,[15] could provide some indication of the structure of the Cu/Aβ complex. Reduction of the most stable Cu(II)/Met complex, **12**, yielding the most stable Cu(I)/Met complex, **23**, the predicted $E°$(**12**/**23**) value was close to that of the aqueous Cu^{2+}/Cu^+ couple, and much lower than that measured for Cu(II)/Aβ. Such a process would require confor-

mational flexibility in Aβ because **12** is compatible with a turn at Met, whereas the backbone of **23** is in the β-strand conformation. If the Met35 region of Aβ was in the β-strand conformation in the oxidized form, the Cu(II)/Aβ complex modeled by **10** would have a somewhat higher reduction potential, but it would still be well below the measured value. We conclude that the Cu(II)/Aβ complex does not have a substantial amount of Cu(II) coordination at the Met35 region of Aβ because none of the structures have a high enough predicted reduction potential.

Acknowledgment. We are grateful to the Alzheimer's Society of Canada and the Natural Sciences and Engineering Research Council (NSERC) of Canada for financial assistance. We also gratefully acknowledge generous allocations of computing resources on the WestGrid systems through the University of Calgary facilities. P.B. acknowledges the Alberta Ingenuity Fund for the provision of a PhD studentship.

Supporting Information Available: Table S1 contains energies, zero-point vibrational energies, thermal corrections, total entropies, number of conformers considered, and free energies of solvation from the theoretical calculations for each species included in this study. Table S2 contains GAUSSIAN archive entries showing B3LYP/6-31G(d) geometries for all species considered in the present work. This material is available free of charge via the Internet at http://pubs.acs.org.

References and Notes

(1) Markesbery, W. R. *Free Radical Biol. Med.* **1997**, *23*, 134−766.

(2) Atwood, C. S.; Huang, X. D.; Moir, R. D.; Tanzi, R. E.; Bush, A. I. *Met. Ions Biol. Syst.* **1999**, *36*, 309−364.

(3) Bush, A. I.; Pettingell, W. H.; Multhaup, G.; Paradis, M. D.; Vonsattel, J. P.; Gusella, J. F.; Beyreuther, K.; Masters, C. L.; Tanzi, R. E. *Science* **1994**, *265*, 1464−1467.

(4) Huang, X.; Atwood C. S.; Moir, R. D.; Hartshorn, M. A.; Vonsattel, J. P.; Tanzi, R. E.; Bush, A. I. *J. Biol. Chem.* **1997**, *272*, 26464−26470.

(5) Atwood, C. S.; Moir, R. D.; Huang, X. D.; Scarpa, R. C.; Bacarra, N. M. E.; Romano, D. M.; Hartshorn, M. K.; Tanzi, R. E.; Bush, A. I. *J. Biol. Chem.* **1998**, *273*, 12817−12826.

(6) Atwood, C. S.; Scarpa, R. C.; Huang, X.; Moir, R. D.; Jones, W. D.; Fairlie, D. P.; Tanzi, R. E.; Bush, A. I. *J. Neurochem.* **2000**, *75*, 1219−1233.

(7) Syme, C. D.; Nadal, R. C.; Rugby, S. E. J.; Viles, J. H. *J. Biol. Chem.* **2004**, *279*, 18169−18177.

(8) Garzón-Rodríguez, W.; Yatsimirsky, A. K.; Glabe, C. G. *Bioorg. Med. Chem. Lett.* **1999**, *9*, 2243−2248.

(9) Garzón-Rodríguez, W.; Sepulveda-Becerra, M.; Milton, S.; Glabe, C. G. *J. Biol. Chem.* **1997**, *272*, 21037−21044.

(10) Ali, F. E. A.; Barnham, K. J.; Barrow, C. J.; Separovic, F. *Aust. J. Chem.* **2004**, *57*, 511−518.

(11) Atwood, C. S.; Perry, G.; Zeng, H.; Kato, Y.; Jones W. D.; Ling, K. Q.; Huang, X.; Moir, R. D.; Wang, D.; Sayre, L. M.; Smith, M. A.; Chen, S. G.; Bush, A. I. *Biochemistry* **2004**, *43*, 560−568.

(12) Miura, T.; Suzuki, K.; Kohata, N.; Takeuchi, H. *Biochemistry* **2000**, *39*, 7024−7031.

(13) Dong, J.; Atwood, C. S.; Anderson, V. E.; Siedlak, S. L.; Smith, M. A.; Perry, G.; Carey P. R. *Biochemistry* **2003**, *42*, 2768−2773.

(14) Raffa, D.; Gómez-Balderas, R.; Rickard, G.; Brunelle, P.; Rauk, A. Submitted for publication.

(15) Huang, X.; Cuajungco, M. P.; Atwood, C. S.; Hartshorn, M. A.; Tyndall, J. D.; Hanson, G. R.; Stokes, K. C.; Leopold, M.; Multhaup, G.; Goldstein, L. E.; Scarpa, R. C.; Saunders, A. J.; Lim, J.; Moir, R. D.; Glabe, C.; Bowden, E. F.; Masters, C. L.; Fairlie, D. P.; Tanzi, R. E.; Bush, A. I. *J. Biol. Chem.* **1999**, *274*, 37111−37116.

(16) Varadarajan, S.; Kañski, J.; Aksenova, M.; Lauderback, C.; Butterfield, D. A. *J. Am. Chem. Soc.* **2001**, *123*, 5625−5631.

(17) Curtain, C. C.; Ali, F.; Volitakis, I.; Cherny, R. A.; Norton, R. S.; Beyreuther, K.; Barrow, C. J.; Masters, C. L.; Bush, A. I.; Barnham, K. J. *J. Biol. Chem.* **2001**, *276*, 20466−20473.

(18) Ciccotosto, G. D.; Tew, D.; Curtain, C. C.; Smith, D.; Carrington, D.; Masters, C. L.; Bush, A. I.; Cherny, R. A.; Cappai, R.; Barnham, K. J. *J. Biol. Chem.* **2004**, *279*, 42528−42534.

(19) Rauk, A.; Armstrong, D. A.; Fairlie, D. P. *J. Am. Chem. Soc.* **2000**, *122*, 9761−9767.

(20) Miller, B. L.; Kuczera, K.; Schöneich, C. *J. Am. Chem. Soc.* **1998**, *120*, 3345−3356.

(21) Brunelle, P.; Rauk, A. *J. Phys. Chem A* **2004**, *108*, 11032−11041.

(22) Hiller, K.-O.; Maslosh, B.; Göbl, M.; Asmus, K.-B. *J. Am. Chem. Soc.* **1981**, *103*, 2734−3743.

(23) It was reported that high concentrations of added phosphate effectively prolonged the lifetime of oxidized Met residues, ref 22.

(24) Frisch, M. J.; Trucks, G. W.; Schlegel, H. B.; Scuseria, G. E.; Robb, M. A.; Cheeseman, J. R.; Zakrzewski, V. G.; Montgomery, J. A., Jr.; Stratmann, R. E.; Burant, J. C.; Dapprich, S.; Millam, J. M.; Daniels, A. D.; Kudin, K. N.; Strain, M. C.; Farkas, O.; Tomasi, J.; Barone, V.; Cossi, M.; Cammi, R.; Mennucci, B.; Pomelli, C.; Adamo, C.; Clifford, S.; Ochterski, J.; Petersson, G. A.; Ayala, P. Y.; Cui, Q.; Morokuma, K.; Malick, D. K.; Rabuck, A. D.; Raghavachari, K.; Foresman, J. B.; Cioslowski, J.; Ortiz, J. V.; Stefanov, B. B.; Liu, G.; Liashenko, A.; Piskorz, P.; Komaromi, I.; Gomperts, R.; Martin, R. L.; Fox, D. J.; Keith, T.; Al-Laham, M. A.; Peng, C. Y.; Nanayakkara, A.; Gonzalez, C.; Challacombe, M.; Gill, P. M. W.; Johnson, B. G.; Chen, W.; Wong, M. W.; Andres, J. L.; Head-Gordon, M.; Replogle, E. S.; Pople, J. A. *Gaussian 98*, revision A.7; Gaussian, Inc.: Pittsburgh, PA, 1998.

(25) Frisch, M. J.; Trucks, G. W.; Schlegel, H. B.; Scuseria, G. E.; Robb, M. A.; Cheeseman, J. R.; Montgomery, Jr., J. A.; Vreven, T.; Kudin, K. N.; Burant, J. C.; Millam, J. M.; Iyengar, S. S.; Tomasi, J.; Barone, V.; Mennucci, B.; Cossi, M.; Scalmani, G.; Rega, N.; Petersson, G. A.; Nakatsuji, H.; Hada, M.; Ehara, M.; Toyota, K.; Fukuda, R.; Hasegawa, J.; Ishida, M.; Nakajima, T.; Honda, Y.; Kitao, O.; Nakai, H.; Klene, M.; Li, X.; Knox, J. E.; Hratchian, H. P.; Cross, J. B.; Bakken, V.; Adamo, C.; Jaramillo, J.; Gomperts, R.; Stratmann, R. E.; Yazyev, O.; Austin, A. J.; Cammi, R.; Pomelli, C.; Ochterski, J. W.; Ayala, P. Y.; Morokuma, K.; Voth, G. A.; Salvador, P.; Dannenberg, J. J.; Zakrzewski, V. G.; Dapprich, S.; Daniels, A. D.; Strain, M. C.; Farkas, O.; Malick, D. K.; Rabuck, A. D.; Raghavachari, K.; Foresman, J. B.; Ortiz, J. V.; Cui, Q.; Baboul, A. G.; Clifford, S.; Cioslowski, J.; Stefanov, B. B.; Liu, G.; Liashenko, A.; Piskorz, P.; Komaromi, I.; Martin, R. L.; Fox, D. J.; Keith, T.; Al-Laham, M. A.; Peng, C. Y.; Nanayakkara, A.; Challacombe, M.; Gill, P. M. W.; Johnson, B.; Chen, W.; Wong, M. W.; Gonzalez, C.; Pople, J. A. *Gaussian 03*, Revision B.05; Gaussian, Inc., Wallingford CT, 2004.

(26) Schaftenaar G.; Noordik, J. H. MOLDEN 4.3. *J. Comput.-Aided Mol. Des.* **2000**, *14*, 123−134.

(27) Flükiger, P.; Lüthi, H. P.; Portmann, S.; Weber J. *MOLEKEL 4.0*; Swiss Center for Scientific Computing: Manno, Switzerland, 2000.

(28) Scott, A. P.; Radom, L. *J. Phys. Chem.* **1996**, *100*, 16502−16513.

(29) (a) Klamt, A.; Schüürmann, G. *J. Chem. Soc., Perkin Trans.* **1993**, *2*, 799−805. (b) Andzelm, J.; Kolmel, C.; Klamt, A. *J. Chem. Phys.* **1995**, *103*, 9312−9320.

(30) Barone, V.; Cossi, M. *J. Phys. Chem. A* **1998**, *102*, 1995−2001.

(31) Cossi, M.; Rega, N.; Scalmani, G.; Barone, V. *J. Comput. Chem.* **2003**, *24*, 669−681.

(32) Zhan, C.; Bentley, J.; Chipman, D. M. *J. Chem. Phys.* **1998**, *108*, 177−192.

(33) Leung, B. O.; Reid, D. L.; Armstrong, D. A.; Rauk, A. *J. Chem. Phys. A* **2004**, *108*, 2720−2725.

(34) Calculated as the difference between $\Delta_f G_{(g)}(H_2O)$ and $\Delta_f G_{(l)}(H_2O)$, corrected to the standard state of 1 M. The calculated value is $\Delta_f G_{solv}(H_2O) = -28.7$ kJ mol^{-1}.

(35) Liptak, M. D.; Gross, K. C.; Seybold, P. G.; Feldgus, S.; Shields, G. C. *J. Am. Chem. Soc.* **2002**, *124*, 6421−6427.

(36) (a) Powell, D. H.; Helm, L.; Merbach, A. E. *J. Chem. Phys.* **1991**, *95*, 9258−9265. (b) Bersuker, I. B. *Chem. Rev.* **2001**, *101*, 1067−1114. (c) Curtiss, L.; Halley, J. W.; Wang, X. R. *Phys. Rev. Lett.* **1992**, *69*, 2435−2438.

(37) (a) Salmon, P. S.; Howells, W. S.; Mills, R. *J. Phys. C: Solid State Phys.* **1987**, *20*, 5727. (b) Powell, D. H.; Helm, L.; Merbach, A. E. *J. Chem Phys.* **1991**, *95*, 9258.

(38) Pasquarello, A.; Petri, I.; Salmon, P. S.; Parisel, O.; Car, R.; Toth, E.; Powell, D. H.; Fischer, H. E.; Helm, L.; Merbach, A. E. *Science* **2001**, *291*, 856−859.

(39) Berces, A.; Nukada, T.; Margl, P.; Ziegler, T. *J. Phys. Chem.* **1999**, *103*, 9693−9701.

(40) Cotton, F. A.; Wilkinson, G. Advanced Inorganic Chemistry, 5th ed.; John Wiley & Sons: New York, 1988; pp 757−766.

(41) Katz, A. K.; Shimoni-Livny, L.; Navon, N.; Bock, C. W.; Glusker J. P. *Helv. Chim. Acta* **2003**, *86*, 1320−1338.

(42) Solomon, E. I.; Szilagyi, R. K.; George, S. D.; Basumallick, L. *Chem. Rev.* **2004**, *104*, 419−458.

(43) Sundberg, R. J.; Martin, R. B. *Chem. Rev.* **1974**, *74*, 471−517.

(44) These −40 kJ mol^{-1} arise from the term $RT \ln[H^+]$, where $[H^+] = 10^{-7}$, all other species for the calculation of $\Delta G_{(aq)}$ are considered to be 1 M.

(45) Rickard, G. A.; Brunelle, P.; Gómez-Balderas, R.; Raffa, D. F.; Rauk, A. Submitted for publication.

(46) Corral, I.; Mó, O.; Yáñez, M. *Int. J. Mass Spectrom.* **2003**, *227*, 401−412.

(47) Corral, I.; Mó, O.; Yáñez, M. *J. Phys. Chem. A* **2003**, *107*, 1370−1376.

(48) Popelier, P. L. A.; Logothetis, G. *J. Organomet. Chem.* **1998**, *555*, 101−111, and references therein.

(49) (a) Foster, J. P.; Weinhold, F. *J. Am. Chem. Soc.* **1980**, *102*, 7211−7218. (b) Reed A. E.; Weinhold, F. *J. Chem. Phys.* **1983**, *78*, 4066−4073. (c) Reed, A. E.; Weinstock, R. B.; Weinhold, F. *J. Chem. Phys.* **1985**, *78*, 735−746.

(50) Burda, J. V.; Pavelka, M.; Simánek, M. *J. Mol. Struct: THEOCHEM* **2004**, *683*, 183−193.

(51) *Handbook of Chemistry and Physics*, 58th ed.; Weast, R. C., Ed.; CRC Press: Boca Raton, FL, 1977−1978.

(52) kJ mol^{-1} is the Gibbs free energy for the half reaction: $^1/_2H_{2(g)} \rightarrow H_{(aq)}^+ + e^-$. It can be obtained from adding $\Delta_f G°_{(g)}(H^+) = 1517$ kJ mol^{-1}, $\Delta G_{solv}(H^+) = -1107$ kJ mol^{-1} (ref 33) and the factor, to change the $H_{(aq)}^+$ reference state to 1 M, $-RT \ln(1/24.6) = 8$ kJ mol^{-1}. Additionally, $\Delta_f G_{(g)}(H^+) = 1517$ kJ mol^{-1} is computed from the $\Delta_f G°_{(g)}(H) = 203$ kJ mol^{-1} (ref 49) plus $\Delta_r G°_{(g)}(H^+ + e^- \rightarrow H) = 1314$ kJ mol^{-1} (Wagman, D. D.; Evans, W. H.; Parker, V. B.; Schumm, R. H.; Halow, I.; Bailey, S. M.; Churney, K. L.; Nuttall, R. L. *J. Phys. Chem. Ref. Data*, *Supl. 1* **1982**, *11*).

(53) Jensen, J. L.; Miller, B. L.; Zhang, X.; Hug, G. L.; Schöneich, C. *J. Am. Chem. Soc.* **1997**, *98*, 9965−9969.

(54) Walter, R. L.; Ealick, S. E.; Friedman, A. M.; Blake, R. C.; Proctor, P.; Shoham, M. *J. Mol. Biol.* **1996**, *263*, 730−751.

(55) Kyritsis, P.; Dennison, C.; Ingledew, W. J.; McFarlane, W.; Sykes, A. G. *Inorg. Chem.* **1995**, *34*, 5370−5374.